



Original Article

A comprehensive analysis for weakly singular nonlinear functional Volterra integral equations using discretization techniques

Imtiyaz Ahmad Bhat^a, Lakshmi Narayan Mishra^{a,*}, Vishnu Narayan Mishra^b,
Mahmoud Abdel-Aty^{c,d}, Montasir Qasymeh^e

^a Department of Mathematics, School of Advanced Sciences, Vellore Institute of Technology, Vellore 632 014, Tamil Nadu, India

^b Department of Mathematics, Indira Gandhi National Tribal University, Lalpur, Amarkantak, Anuppur, 484 887, Madhya Pradesh, India

^c Jadara Research Center, Jadara University, P.O. Box 733, Irbid, 21110, Jordan

^d Deanship of Graduate Studies and Research, Ahlia University, Manama, 10878, Bahrain

^e Department of Electrical Engineering, Abu Dhabi University, Abu Dhabi, 59911, United Arab Emirates

ARTICLE INFO

MSC:

65R20

26A33

45G10

65G99

Keywords:

Nonlinear integral equations

Functional integral equations

Fixed point theorem

Trapezoidal and Euler methods

Grönwall inequality

ABSTRACT

This study investigates weakly singular nonlinear functional Volterra integral equations (WSNFVIEs) of Urysohn type involving Riemann–Liouville operator. By imposing specific smoothness conditions on the involved functions, we establish both the existence and uniqueness of the solution using a fixed point approach. Subsequently, we employ discretization methods such as the trapezoidal and Euler methods to approximate the solution, resulting in a system of nonlinear algebraic equations. To ascertain the convergence order of the Euler method (first order) and the trapezoidal method (second order), we utilize the Grönwall inequality and its discrete counterpart. Additionally, we introduce a novel Grönwall inequality to establish the convergence of the trapezoidal method. Thoroughly we examine the Hyers–Ulam–Rassias and Hyers–Ulam stability of the integral equations within the specified domain. Finally, the efficacy of the proposed methods is validated through numerical examples accompanied by comparative analyses.

1. Introduction

The present article discusses the WSNFVIEs of the Urysohn type

$$\phi(\rho) = \varpi(\rho) + \chi \left(\rho, \frac{1}{\Gamma(\alpha)} \int_0^\rho (\rho - \mu)^{\alpha-1} \mathfrak{R}(\rho, \mu, \phi(\mu)) d\mu \right), \quad \rho \in [0, \kappa], \quad (1.1)$$

where, $0 < \alpha < 1$, $0 < \kappa < \infty$, and $\varpi : [0, \kappa] \rightarrow \mathbb{R}$, $\chi : [0, \kappa] \times \mathbb{R} \rightarrow \mathbb{R}$ and $\mathfrak{R} : [0, \kappa]^2 \times \mathbb{R} \rightarrow \mathbb{R}$, are given continuous functions, $\phi(\rho)$ is the unknown solution function which is to be determined. The integral equation (1.1) is the generalization of the Hammerstein type integral equation.

Integral equations of functional type appear in several kinds of forms and are considered to be a distinctive and intriguing area of nonlinear analysis. They exhibit an array of concerns that are prevalent in daily life and are known by many different labels. These equations are of significant importance in applied mathematics, particularly nonlinear ones, as evidenced by their increasing integration into various fields such as biology, economics, traffic theory and acoustic scattering, optimal control theory, kinetic theory of gases, etc. [1–5].

Integral equations of both types singular as well as weakly singular are of notable significance, particularly in addressing inverse boundary value problems occurring within domains characterized by fractal curves, where conventional calculus methodologies are inadequate. Extensive examination has been devoted to Abel equations and analogous fractional order integral equations, owing to their wide-ranging utility in modelling phenomena across domains such as viscoelasticity, electrical circuits and biophysics. Mathematical models serve as powerful instruments for examining diverse real-world scenarios. Scholars have utilized algebraic, integral, and differential equations to construct mathematical models for the stated objectives [6–8]. Integral equations featuring weakly singular kernels, as described in (1.1) are encountered in various scientific and technological domains, including chemical reactions and mathematical physics. These equations play essential roles in diverse applications such as heat radiation, stereology, heat conduction having boundary conditions mixed, crystal growth, gas absorption, superfluidity [9–13].

* Corresponding author.

E-mail addresses: imtiyaz.ahmad@vit.ac.in (I.A. Bhat), lakshminarayan.mishra@vit.ac.in (L.N. Mishra), vnm@igtntu.ac.in (V.N. Mishra), mabdelaty@ahlia.edu.bh (M. Abdel-Aty), montasir.qasymeh@adu.ac.ae (M. Qasymeh).

<https://doi.org/10.1016/j.aej.2024.08.017>

Received 9 December 2023; Received in revised form 15 April 2024; Accepted 3 August 2024

Available online 12 August 2024

1110-0168/© 2024 The Authors. Published by Elsevier B.V. on behalf of Faculty of Engineering, Alexandria University. This is an open access article under the CC BY-NC-ND license (<http://creativecommons.org/licenses/by-nc-nd/4.0/>).

The solvability and characteristics of singular Volterra integral equations and their existence of solutions have been investigated employing diverse analytical and approximation methods. For example, in [14], the authors demonstrated the approximate solution by applying the Galerkin and the iterated form of Galerkin methods and also establish the methods convergence analysis of the Hammerstein type weakly singular Volterra integral equation of the form

$$\phi(\rho) - \int_0^\rho h(y, \mu)\mathfrak{K}(\mu, \phi(\mu))d\mu = \varpi(\rho), \quad \rho \in [0, 1], \tag{1.2}$$

where kernel is

$$h(y, \mu) = \hat{h}(y, \mu)|y - \mu|^{-\alpha}, \quad 0 < \alpha < 1. \tag{1.3}$$

. Furthermore, the authors of [15] discussed multi-domain hybrid type spectral collocation technique of hp -version to the integral equation of the form

$$\phi(\rho) = \varpi(\rho) + \int_0^\rho (\rho - \mu)^\alpha \mathfrak{K}(\rho, \mu, \phi(\mu))d\mu, \quad \rho \in [0, \kappa], \quad 0 < \alpha < 1, \tag{1.4}$$

to explore the numerical solution containing the possible singularity at $\rho = 0$. Also, the iterated method has been used to approximate the numerical solution of an integral equation

$$\phi(\rho) = \varpi(\rho) + \int_0^\rho (\rho - \mu)^{\alpha-1} \mathfrak{K}(\rho, \mu, \phi(\mu))d\mu, \quad \rho \in [0, \kappa], \quad 0 < \alpha < 1, \tag{1.5}$$

where $\varpi : (0, \kappa] \rightarrow \mathbb{R}$, which has been discussed in [16]. While as the same integral equation has been discussed in [17] having non-smooth solution at initial point. The numerical solution of (1.5) has also been explored in [18] employing an iterated based projection technique in connection with rationalized Haar wavelets. The approximate solution of nonlinear integral equation

$$\phi(\rho) = \varpi(\rho) + \frac{\Psi(\rho)}{\Gamma(\alpha)} \int_0^\rho (\rho - \mu)^{\alpha-1} \zeta(\mu)\mathcal{H}(\phi(\mu))d\mu, \quad \rho \in [0, \kappa], \quad \alpha > 0, \tag{1.6}$$

and its existence have been investigated in [19]. The authors also discussed the stability analysis of the considered integral equations in the space of $C([0, \kappa], \mathbb{R})$.

In addition, numerous references have covered the subject of functional integral equations and their existence of solutions. For example, the existence of the solution to integral equation

$$\phi(\rho) = \varpi(\rho, \phi(\rho)) + \chi \left(\rho, \int_0^\rho \mathfrak{K}(\rho, \mu, \phi(\rho))d\mu, \phi(\alpha(\rho)) \right), \quad \rho \in [0, \hat{a}], \tag{1.7}$$

in Banach algebra by using the technique of measure of noncompactness in the framework of Darbo’s fixed point theorem has been discussed in [20].

However, for nonlinear functional integral equations, the investigation of numerical techniques is still in the early stages and there have not been many studies in this field [21–28]. This is compared to the abundance of research on the numerical investigation of classical integral equations (see, [29–36]). Generally, the exact solution to these equations is not always attainable, even in cases where the existence of a single possible solution is established. In addition to that, numerous practical scenarios described by integral equations, the kernels exhibit a lack of smoothness, posing challenges in both finding and numerically approximating solutions. Traditional analytical techniques, such as projection methods, falter in such instances due to the resulting ill-conditioned linear systems and the complexity of convergence and error analysis, often necessitating laborious approaches when standard calculus techniques are inapplicable. Moreover, these methods frequently entail high implementation costs. Consequently, there is a pressing demand for efficient and user-friendly numerical approaches tailored to address these equation types. Thus, we resort to numerical approaches to provide an accurate approximation of the solution.

The aforementioned works encouraged us and drove our study, which we used to present a thorough analysis of discretization methods for the Urysohn type nonlinear functional weakly singular Volterra integral equations to extend and improve the current findings in the literature. To the very best of the authors’ knowledge, this work provides the first address on numerical techniques for solving functional Eq. (1.1).

In our pursuit, we initially set forth hypotheses to guarantee the unique solution of (1.1) within the designated space $\mathfrak{B} = \mathcal{L}^\infty[0, \kappa]$. Specifically, we demonstrate that, under appropriate conditions, the operator \mathcal{T} defined in (3.3) effectively maintains the properties of \mathfrak{B} , thereby ensuring that all solutions to (1.1) remain confined within this domain. Furthermore, through additional assumptions and the application of the Banach fixed point principle, we establish the unique existence of the solution to (1.1) within \mathfrak{B} . Lastly, by employing the proposed methods, we streamline the solution process for (1.1) into a series of nonlinear algebraic equations.

The study is organized as follows: Commencing with Section 2, some important definitions, notations and theorems have been discussed. In Section 3 a rigorous investigation is conducted into the existence and uniqueness of a solution to the integral Eq. (1.1) and conduct a thorough investigation into the stability properties of Hyers–Ulam–Rassias (H-U-R) and Hyers–Ulam (H-U) in relation to integral equations involving the Riemann–Liouville operator within the designated spatial framework. Section 4, undertakes the discretization of the equation via Euler’s and trapezoidal methods, transforming it into a system of nonlinear equations. The subsequent establishment of the order of convergence for both methods is substantiated through the application of Grönwall inequality and its discrete manifestation. Section 5 examines the practicality of the methods, substantiated by an empirical foundation through numerical examples and comparative analyses. Culminating our exploration in Section 6, provides a comprehensive set of conclusions, encapsulating the essence and implications derived from the preceding sections.

2. Preliminaries

This section introduces some notations and background details essential for explaining our primary outcomes. Let \mathbb{R} denotes the set of all real numbers, and define $\mathfrak{B} = \mathcal{L}^\infty([0, \kappa], \mathbb{R})$ as the space of all essentially bounded functions, $\phi : [0, \kappa] \rightarrow \mathbb{R}$, where $0 < \kappa < \infty$. Hence, the pair $(\mathfrak{B}, \|\cdot\|_\infty)$ forms a Banach space with the norm $\|\phi\|_\infty = \text{ess sup}\{|\delta(\rho)|, \rho \in [0, \kappa]\}$.

Notations used:

- EM: Euler’s method;
- TM: Trapezoidal method;
- VIO: Volterra integral operator;
- $C^n([a, b])$: Set of all n th times continuously differentiable functions on interval $[a, b]$;
- In this work, it is supposed that when $\dot{m}_1 \geq \dot{m}_2$, $\sum_{\dot{m}_1}^{\dot{m}_2}$ equals to zero.

Definition 2.1 ([19]). The fractional integral of a function $\phi(\rho)$ of order $\alpha > 0$, as formulated by the Riemann–Liouville, is defined as follows:

$${}^\alpha \mathcal{I}_0^\rho \phi(\rho) = \frac{1}{\Gamma(\alpha)} \int_0^\rho (\rho - \mu)^{\alpha-1} \phi(\mu)d\mu, \tag{2.1}$$

where $\Gamma(\alpha) = \int_0^\infty e^{-v}v^{\alpha-1}dv$, ensuring that the right-hand side is valid for each point within the interval $[0, \infty)$.

Definition 2.2 ([19]). If for every function $\phi \in \mathfrak{B}$ satisfying

$$\left| \phi(\rho) - \varpi(\rho) - \chi \left(\rho, \frac{1}{\Gamma(\alpha)} \int_0^\rho (\rho - \mu)^{\alpha-1} \mathfrak{K}(\rho, \mu, \phi(\mu))d\mu \right) \right| \leq y(\rho), \tag{2.2}$$

where the function $y(\rho)$ is nonnegative, there exists $\phi^* \in \mathfrak{B}$ a solution to (1.1) such that $|\phi^*(\rho) - \phi(\rho)| < \epsilon y(\rho)$ holds for each ρ , where $\epsilon > 0$

and is independent of ϕ and ϕ^* , then (1.1) possesses H-U-R stability relative to $y(\rho)$.

Also, if the function $y(\rho)$ in (2.2) is any constant, then (1.1) possesses H-U stability.

Theorem 2.3 [37]. Consider a nonnegative constant ζ and two nonnegative integrable functions, f and g . If

$$f(u) \leq \zeta + \int_0^u g(v)f(v)dv, \quad v \geq 0,$$

then

$$f(u) \leq \zeta \exp\left(\int_0^u g(v)dv\right), \quad v \geq 0.$$

Theorem 2.4 [37]. Assume that the sequences $\{\gamma_{\bar{m}}\}$, $\{p_{\bar{m}}\}$ and $\{q_{\bar{m}}\}$ are nonnegative, such that

$$\gamma_{\bar{m}} \leq p_{\bar{m}} + \sum_{0 \leq i < \bar{m}} q_i \gamma_i, \quad \bar{m} \geq 0,$$

then

$$\begin{aligned} \gamma_{\bar{m}} &\leq p_{\bar{m}} + \sum_{0 \leq i < \bar{m}} q_i \gamma_i \prod_{i < j < \bar{m}} (1 + q_j) \\ &\leq p_{\bar{m}} + \sum_{0 \leq i < \bar{m}} q_i \gamma_i \left(\exp \sum_{i < j < \bar{m}} q_j \right). \end{aligned}$$

The following lemma recalls two quadrature rules:

Lemma 2.5. Assume that the interval $[c, d]$ is split into \bar{m} subintervals, each with a length of $\delta = (d - c)/\bar{m}$.

(1) If $u \in C^1[c, d]$, then

$$\int_c^d u(\rho)d\rho = \delta \sum_{i=0}^{\bar{m}-1} u(c + i\delta) + \frac{\delta}{2}(d - c)u'(\eta), \quad \eta \in (c, d). \quad (2.3)$$

(2) If $u \in C^2[c, d]$, then

$$\int_c^d u(\rho)d\rho = \delta \sum_{i=0}^{\bar{m}-1} u(c + i\delta) + \frac{\delta^2}{12}(d - c)u''(\eta), \quad \eta \in (c, d). \quad (2.4)$$

Proof. For proof, see the articles [38,39] for part (1) and (2), respectively. \square

3. Existence and uniqueness of solution

This section examines the existence of the solution to the integral Eq. (1.1) and its uniqueness. For this, let us carry out the modification of (1.1) in an operator form:

$$\phi(\rho) = \varpi(\rho) + (\mathcal{F}\hat{K}\phi)(\rho) = \varpi(\rho) + \chi(\rho, (\hat{K}\phi)(\rho)),$$

where

$$(\hat{K}\phi)(\rho) = \frac{1}{\Gamma(\alpha)} \int_0^\rho (\rho - \mu)^{\alpha-1} \mathfrak{K}(\rho, \mu, \phi(\mu))d\mu,$$

is termed as VIO and $(\mathcal{F}\phi)(\rho) = \chi(\rho, \phi(\rho))$, the Nemytskii operator [40]. Also, suppose that:

(E₁) $\phi \in \mathfrak{B}$.

(E₂) $(\mathcal{F}\hat{K}0)(\rho) = \chi(\rho, (\hat{K}0)(\rho)) = \chi\left(\rho, \frac{1}{\Gamma(\alpha)} \int_0^\rho (\rho - \mu)^{\alpha-1} \mathfrak{K}(\rho, \mu, 0) d\mu\right) \in \mathfrak{B}$ and the Lipschitz condition for a Lipschitz constant $\gamma_1 > 0$ is satisfied by χ according to its second parameter as

$$|\chi(\rho, v_1) - \chi(\rho, v_2)| \leq \gamma_1 |v_1 - v_2|, \quad \rho \in [0, \kappa], v_1, v_2 \in \mathbb{R}, \quad (3.1)$$

(E₃) The Lipschitz condition for a Lipschitz constant $\gamma_2 > 0$ is satisfied by the kernel \mathfrak{K} according to its third parameter as

$$|\mathfrak{K}(\rho, \mu, \omega_1) - \mathfrak{K}(\rho, \mu, \omega_2)| \leq \gamma_2 |\omega_1 - \omega_2|, \quad \rho \in [0, \kappa], \omega_1, \omega_2 \in \mathbb{R}, \quad (3.2)$$

(E₄) The VIO \hat{K} is bounded, i.e., there exists a constant $Q > 0$ such that $\|\hat{K}\|_\infty \leq Q$.

(E₅) $\left(\frac{\gamma_1 \gamma_2 \kappa^\alpha}{\Gamma(\alpha+1)}\right) < 1$.

Remark 3.1. Supposition (E₂) is similar to:

For a specific constant γ_1 , the function χ demonstrates a continuous and bounded first partial derivative with respect to v , i.e.,

$$\sup_v \left| \frac{\partial \chi}{\partial v} \right| \leq \gamma_1.$$

Remark 3.2. Supposition (E₃) is similar to:

For a specific constant γ_2 , the function \mathfrak{K} demonstrates a continuous and bounded first partial derivative with respect to ω , i.e.,

$$\sup_\omega \left| \frac{\partial \mathfrak{K}}{\partial \omega} \right| \leq \gamma_2.$$

The subsequent theorem ensures the solution's existence and uniqueness in \mathfrak{B} to (1.1).

Theorem 3.3. There is a unique solution $\phi \in \mathfrak{B}$ to (1.1), if (E₁)–(E₅) hold.

Proof. To establish the proof of the theorem, (1.1) can be represented as fixed point problem

$$\phi = \mathcal{T}\phi, \quad (\mathcal{T}\phi)(\rho) = \varpi(\rho) + (\mathcal{F}\hat{K}\phi)(\rho). \quad (3.3)$$

Now, we have to prove that \mathcal{T} maps \mathfrak{B} to itself. To prove this, let $\phi \in \mathfrak{B}$ be arbitrary, then from the condition (E₂) and (3.3), we have

$$\begin{aligned} |(\mathcal{T}\phi)(\rho)| &= \left| \varpi(\rho) + \chi(\rho, (\hat{K}\phi)(\rho)) \right| \\ &= \left| \varpi(\rho) + \chi(\rho, (\hat{K}\phi)(\rho)) + \chi(\rho, 0) - \chi(\rho, 0) \right| \\ &\leq \left| \varpi(\rho) \right| + \left| \chi(\rho, (\hat{K}\phi)(\rho)) - \chi(\rho, 0) \right| + \left| \chi(\rho, 0) \right| \\ &\leq \left| \varpi(\rho) \right| + \gamma_1 \left| (\hat{K}\phi)(\rho) \right| + \left| \chi(\rho, 0) \right| \\ &\leq \|\varpi\|_\infty + \gamma_1 \|\hat{K}\phi\|_\infty + \|\chi(\rho, 0)\|_\infty \\ &\leq \|\varpi\|_\infty + \gamma_1 \|\hat{K}\|_\infty \|\phi\|_\infty + \|\chi(\rho, 0)\|_\infty, \quad \forall \rho \in [0, \kappa], \end{aligned}$$

so in light of (E₁), (E₂) and (E₄), $\|(\mathcal{T}\phi)\|_\infty < \infty$, it follows \mathcal{T} maps \mathfrak{B} to itself.

Now, we have to prove that \mathcal{T} is contraction. Let $\phi_1, \phi_2 \in \mathfrak{B}$ be arbitrary, then from (E₂) and (E₃), we obtain

$$\begin{aligned} |(\mathcal{T}\phi_1)(\rho) - (\mathcal{T}\phi_2)(\rho)| &\leq \left| \chi\left(\rho, \frac{1}{\Gamma(\alpha)} \int_0^\rho (\rho - \mu)^{\alpha-1} \mathfrak{K}(\rho, \mu, \phi_1(\mu))d\mu\right) \right. \\ &\quad \left. - \chi\left(\rho, \frac{1}{\Gamma(\alpha)} \int_0^\rho (\rho - \mu)^{\alpha-1} \mathfrak{K}(\rho, \mu, \phi_2(\mu))d\mu\right) \right| \\ &\leq \frac{\gamma_1}{\Gamma(\alpha)} \int_0^\rho (\rho - \mu)^{\alpha-1} \left| \mathfrak{K}(\rho, \mu, \phi_1(\mu)) - \mathfrak{K}(\rho, \mu, \phi_2(\mu)) \right| d\mu \\ &\leq \frac{\gamma_1 \gamma_2}{\Gamma(\alpha)} \int_0^\rho (\rho - \mu)^{\alpha-1} \left| \phi_1(\mu) - \phi_2(\mu) \right| d\mu \\ &\leq \frac{\gamma_1 \gamma_2}{\Gamma(\alpha)} \|\phi_1 - \phi_2\|_\infty \int_0^\rho (\rho - \mu)^{\alpha-1} d\mu \\ &\leq \frac{\gamma_1 \gamma_2 \kappa^\alpha}{\Gamma(\alpha+1)} \|\phi_1 - \phi_2\|_\infty \\ &\leq C \|\phi_1 - \phi_2\|_\infty, \text{ where } C = \frac{\gamma_1 \gamma_2 \kappa^\alpha}{\Gamma(\alpha+1)}. \end{aligned}$$

Based on the assumption (E₅), it can be concluded that \mathcal{T} exhibits contraction properties. As a result, the conclusion can be drawn by applying the Banach fixed point theorem. \square

Theorem 3.4. Suppose that conditions (E₁)–(E₅) hold for (1.1). Also, let $\phi \in \mathfrak{B}$ is such that

$$\left| \phi(\rho) - \varpi(\rho) - \chi \left(\rho, \frac{1}{\Gamma(\alpha)} \int_0^\rho (\rho - \mu)^{(\alpha-1)} \mathfrak{K}(\rho, \mu, \phi(\mu)) d\mu \right) \right| \leq y(\rho), \quad (3.4)$$

where the function $y(\rho)$ is nonnegative. Then (1.1) possesses H-U-R stability relative to $y(\rho)$.

Proof. Following Theorem 3.3, there is only one solution $\phi^*(\rho) \in \mathfrak{B}$.

Assume that $\phi \in \mathfrak{B}$ be such that

$$\left| \phi(\rho) - \varpi(\rho) - \chi \left(\rho, \frac{1}{\Gamma(\alpha)} \int_0^\rho (\rho - \mu)^{(\alpha-1)} \mathfrak{K}(\rho, \mu, \phi(\mu)) d\mu \right) \right| \leq y(\rho). \quad (3.5)$$

Now, in consideration of Definition (2.2), for each $\rho \in [0, \kappa]$, we proceed as

$$\begin{aligned} |\phi(\rho) - \phi^*(\rho)| &= \left| \phi(\rho) - \varpi(\rho) - \chi \left(\rho, \frac{1}{\Gamma(\alpha)} \int_0^\rho (\rho - \mu)^{(\alpha-1)} \mathfrak{K}(\rho, \mu, \phi(\mu)) d\mu \right) \right| \\ &= \left| \phi(\rho) - \varpi(\rho) - \chi \left(\rho, \frac{1}{\Gamma(\alpha)} \int_0^\rho (\rho - \mu)^{(\alpha-1)} \mathfrak{K}(\rho, \mu, \phi(\mu)) d\mu \right) \right. \\ &\quad + \chi \left(\rho, \frac{1}{\Gamma(\alpha)} \int_0^\rho (\rho - \mu)^{(\alpha-1)} \mathfrak{K}(\rho, \mu, \phi(\mu)) d\mu \right) \\ &\quad \left. - \chi \left(\rho, \frac{1}{\Gamma(\alpha)} \int_0^\rho (\rho - \mu)^{(\alpha-1)} \mathfrak{K}(\rho, \mu, \phi^*(\mu)) d\mu \right) \right| \\ &\leq \left| \phi(\rho) - \varpi(\rho) - \chi \left(\rho, \frac{1}{\Gamma(\alpha)} \int_0^\rho (\rho - \mu)^{(\alpha-1)} \mathfrak{K}(\rho, \mu, \phi(\mu)) d\mu \right) \right| \\ &\quad + \left| \chi \left(\rho, \frac{1}{\Gamma(\alpha)} \int_0^\rho (\rho - \mu)^{(\alpha-1)} \mathfrak{K}(\rho, \mu, \phi(\mu)) d\mu \right) \right. \\ &\quad \left. - \chi \left(\rho, \frac{1}{\Gamma(\alpha)} \int_0^\rho (\rho - \mu)^{(\alpha-1)} \mathfrak{K}(\rho, \mu, \phi^*(\mu)) d\mu \right) \right| \\ &\leq y(\rho) + \frac{\gamma_1}{\Gamma(\alpha)} \int_0^\rho (\rho - \mu)^{(\alpha-1)} \left| \mathfrak{K}(\rho, \mu, \phi(\mu)) - \mathfrak{K}(\rho, \mu, \phi^*(\mu)) \right| d\mu \\ &\leq y(\rho) + \frac{\gamma_1 \gamma_2}{\Gamma(\alpha)} \int_0^\rho (\rho - \mu)^{(\alpha-1)} |\phi(\mu) - \phi^*(\mu)| d\mu \\ &\leq y(\rho) + \frac{\gamma_1 \gamma_2}{\Gamma(\alpha)} \|\phi(\mu) - \phi^*(\mu)\|_\infty \int_0^\rho (\rho - \mu)^{(\alpha-1)} d\mu \\ &\leq y(\rho) + \frac{\gamma_1 \gamma_2 \kappa^\alpha}{\Gamma(\alpha + 1)} \|\phi(\mu) - \phi^*(\mu)\|_\infty \\ &\leq y(\rho) + C \|\phi(\mu) - \phi^*(\mu)\|_\infty, \text{ where } C = \frac{\gamma_1 \gamma_2 \kappa^\alpha}{\Gamma(\alpha + 1)}. \end{aligned}$$

Thus, $|\phi(\rho) - \phi^*(\rho)| \leq \|\phi(\rho) - \phi^*(\rho)\|_\infty \leq y(\rho) + C \|\phi(\mu) - \phi^*(\mu)\|_\infty$, implies that $|\phi(\rho) - \phi^*(\rho)| \leq \|\phi(\rho) - \phi^*(\rho)\|_\infty \leq D y(\rho)$, where $D = \frac{1}{1-C} > 0$, as $C < 1$. Therefore, about $y(\rho)$, (1.1) exhibits H-U-R stability. \square

Theorem 3.5. Suppose that conditions (E₁)–(E₅) hold for (1.1). Also, let $\phi \in \mathfrak{B}$ is such that

$$\left| \phi(\rho) - \varpi(\rho) - \chi \left(\rho, \frac{1}{\Gamma(\alpha)} \int_0^\rho (\rho - \mu)^{(\alpha-1)} \mathfrak{K}(\rho, \mu, \phi(\mu)) d\mu \right) \right| \leq \epsilon, \quad (3.6)$$

where $\epsilon > 0$. Then (1.1) possesses H-U stability relative to ϵ .

Proof. In a similar manner, we can demonstrate this theorem by using the value of $y(\rho) = \epsilon$ in Theorem 3.4, where $\epsilon > 0$. \square

4. Analysis and convergence of numerical methods

The focus of this section is to discuss the analysis and convergence of the discretization techniques (Euler and trapezoidal) applied to solve (1.1).

Let us define $\delta = \frac{\kappa}{\mathcal{M}}$, where \mathcal{M} is a positive integer and let the Θ_δ be the grid points defined as

$$\Theta_\delta = \{\rho_{\dot{m}} = \dot{m}\delta : \dot{m} = 0, \dots, \mathcal{M}\},$$

also, let the corresponding grid functions be $\{\phi_{\dot{m}}\}$.

4.1. Euler method

Employing the Euler method, for a defined grid function $\phi_{\dot{m}}$, which must satisfy the difference scheme as follows:

$$\phi_{\dot{m}} = \varpi_{\dot{m}} + \chi \left(\rho_{\dot{m}}, \frac{1}{\Gamma(\alpha)} \delta \sum_{i=0}^{\dot{m}-1} \frac{\mathfrak{K}(\rho_{\dot{m}}, \rho_i, \phi_i)}{(\rho_{\dot{m}} - \rho_i)^{1-\alpha}} \right), \quad (4.1)$$

with $\varpi_{\dot{m}} = \varpi(\rho_{\dot{m}})$, $\dot{m} = 0, \dots, \mathcal{M}$.

Theorem 4.1. Suppose that corresponding to μ , ϕ , and μ , the continuously differentiable functions are \mathfrak{K} and ϕ , respectively. Then the Euler method (4.1), converges with a linear rate of convergence, to the unique solution of (1.1) only if the suppositions (E₁)–(E₃) hold.

Proof. Putting (1.1) on Θ_δ produces

$$\phi(\rho_{\dot{m}}) = \varpi(\rho_{\dot{m}}) + \chi \left(\rho_{\dot{m}}, \frac{1}{\Gamma(\alpha)} \int_0^{\rho_{\dot{m}}} \frac{\mathfrak{K}(\rho_{\dot{m}}, \mu, \phi(\mu))}{(\rho_{\dot{m}} - \mu)^{1-\alpha}} d\mu \right). \quad (4.2)$$

Now, applying Lemma 2.5 and the continuity of \mathfrak{K} and ϕ , the following is the form of (4.1)

$$\phi(\rho_{\dot{m}}) = \varpi(\rho_{\dot{m}}) + \chi \left(\rho_{\dot{m}}, \frac{1}{\Gamma(\alpha)} \delta \sum_{i=0}^{\dot{m}-1} \frac{\mathfrak{K}(\rho_{\dot{m}}, \rho_i, \phi(\rho_i))}{(\rho_{\dot{m}} - \rho_i)^{1-\alpha}} + \varrho_{\dot{m}} \right), \quad \rho_{\dot{m}} \in \Theta_\delta, \quad (4.3)$$

where $\varrho_{\dot{m}} = \frac{\delta \rho_{\dot{m}}}{2} \frac{\partial}{\partial \mu} \mathfrak{K}(\rho_{\dot{m}}, \mu, \phi(\mu)) \Big|_{\mu=\rho_{\dot{m}}'} = \mathcal{O}(\delta)$, for some $\rho_{\dot{m}}' \in (0, \rho_{\dot{m}})$.

Subtracting Eq. (4.1) from (4.3), we obtain

$$\begin{aligned} \phi(\rho_{\dot{m}}) - \phi_{\dot{m}} &= \chi \left(\rho_{\dot{m}}, \frac{1}{\Gamma(\alpha)} \delta \sum_{i=0}^{\dot{m}-1} \frac{\mathfrak{K}(\rho_{\dot{m}}, \rho_i, \phi(\rho_i))}{(\rho_{\dot{m}} - \rho_i)^{1-\alpha}} + \varrho_{\dot{m}} \right) \\ &\quad - \chi \left(\rho_{\dot{m}}, \frac{1}{\Gamma(\alpha)} \delta \sum_{i=0}^{\dot{m}-1} \frac{\mathfrak{K}(\rho_{\dot{m}}, \rho_i, \phi_i)}{(\rho_{\dot{m}} - \rho_i)^{1-\alpha}} \right), \\ &\quad \dot{m} = 0, \dots, \mathcal{M}. \end{aligned} \quad (4.4)$$

For $\dot{m} = 0, \dots, \mathcal{M}$, using (4.4) as modulus, let

$$e_{\dot{m}} = |\phi(\rho_{\dot{m}}) - \phi_{\dot{m}}|, \quad (4.5)$$

in light of the triangle inequality and hypotheses (E₂) and (E₃), we obtain

$$e_{\dot{m}} \leq \sum_{i=0}^{\dot{m}-1} \frac{\gamma_1 \gamma_2}{\Gamma(\alpha) (\rho_{\dot{m}} - \rho_i)^{1-\alpha}} \delta e_i + \gamma_1 |\varrho_{\dot{m}}|. \quad (4.6)$$

Using Eq. (4.6) and Theorem 2.4, let $q = \frac{1}{(\rho_{\dot{m}} - \rho_i)^{1-\alpha}}$, such that $\sum_{i=0}^{\dot{m}-1} q_i \approx 1$ and $P = \frac{\gamma_1 \gamma_2}{\Gamma(\alpha)}$, we can now deduce that

$$\begin{aligned} e_{\dot{m}} &\leq \gamma_1 |\varrho_{\dot{m}}| + \sum_{i=0}^{\dot{m}-1} (\gamma_1 |\varrho_i|) (q_i P \delta) \left(\exp \sum_{i < j < \dot{m}} q_j P \delta \right) \\ &= \gamma_1 |\varrho_{\dot{m}}| + \gamma_1 P \delta \sum_{i=0}^{\dot{m}-1} |\varrho_i| q_i e^{(\dot{m}-i)\delta} \\ &= \gamma_1 |\varrho_{\dot{m}}| + \delta \gamma_1 P e^{\dot{m}\delta} \sum_{i=0}^{\dot{m}-1} |\varrho_i| \\ &= \gamma_1 |\varrho_{\dot{m}}| + \delta \gamma_1 P e^{\dot{m}\delta} \sum_{i=0}^{\dot{m}-1} |\varrho_i| \\ &= \gamma_1 |\varrho_{\dot{m}}| + \delta \gamma_1 P e^{\mathcal{M}\kappa} \sum_{i=0}^{\dot{m}-1} |\varrho_i|, \quad \dot{m} = 0, \dots, \mathcal{M}. \end{aligned}$$

Since $|\varrho_i| = \mathcal{O}(\delta)$, for $j = 0, \dots, \mathcal{M}$, hence proves the first order convergence of EM's. \square

4.2. Trapezoidal method

The system of nonlinear equations given below must be met for $\dot{m} = 0, \dots, \mathcal{M}$ to utilize the trapezoidal approach to obtain an approximate

solution $\phi_{\dot{m}}$ to the problem:

$$\phi_{\dot{m}} = \varpi_{\dot{m}} + \chi \left(\rho_{\dot{m}}, \frac{1}{\Gamma(\alpha)} \frac{\delta}{2} \sum_{i=0}^{\dot{m}} \left[\frac{\mathfrak{R}(\rho_{\dot{m}}, \rho_{i-1}, \phi_{i-1})}{(\rho_{\dot{m}} - \rho_{i-1})^{1-\alpha}} + \frac{\mathfrak{R}(\rho_{\dot{m}}, \rho_i, \phi_i)}{(\rho_{\dot{m}} - \rho_i)^{1-\alpha}} \right] \right), \quad (4.7)$$

with $\phi_{\dot{m}} = \phi(\rho_{\dot{m}})$.

We now prove the following lemma, which is a discrete version of the Grönwall inequality that we will require later.

Lemma 4.2. For an indexed set $\mathcal{U}_{\dot{m}}$, consider $\mathcal{U} = \max |\mathcal{U}_{\dot{m}}|$. Let us assume that the nonnegative grid functions are $\vartheta_{\dot{m}}$. If $\vartheta_{\dot{m}}$ satisfies the following inequality for a constant $D > 0$, i.e.,

$$\vartheta_{\dot{m}} \leq \frac{\delta}{2} D \sum_{i=0}^{\dot{m}} (\vartheta_{i-1} + \vartheta_i) + \mathcal{U}_{\dot{m}}, \quad \dot{m} = 0, \dots, \mathcal{M}, \quad (4.8)$$

then

$$\vartheta_{\dot{m}} \leq \mathcal{U} e^{D\kappa}, \quad \dot{m} = 0 \dots, \mathcal{M}.$$

Proof. For $\dot{m} = 0, \dots, \mathcal{M}$, we have from (4.8) as follows:

$$\vartheta_{\dot{m}} \leq \frac{D}{2} \sum_{i=0}^{\dot{m}} \left[\int_{\rho_{i-2}}^{\rho_{i-1}} \vartheta_{i-1} d\rho + \int_{\rho_{i-1}}^{\rho_i} \vartheta_i d\rho \right] + \mathcal{U}_{\dot{m}}, \quad (4.9)$$

for a piecewise constant function defined as

$$\phi(\rho) = \vartheta_i, \quad \rho \in (\rho_{i-1}, \rho),$$

then, we have from (4.9) the form as

$$\phi(\rho_{\dot{m}}) \leq \frac{D}{2} \sum_{i=0}^{\dot{m}} \left[\int_{\rho_{i-2}}^{\rho_{i-1}} \phi(\mu) d\mu + \int_{\rho_{i-1}}^{\rho_i} \phi(\mu) d\mu \right] + \mathcal{U}_{\dot{m}}. \quad (4.10)$$

Let, if $\phi(\rho) = 0$, for $\rho \notin [0, \kappa]$, then from (4.10), we obtain

$$\phi(\rho_{\dot{m}}) \leq \frac{D}{2} \left[\int_0^{\rho_{\dot{m}-1}} \phi(\mu) d\mu + \int_0^{\rho_{\dot{m}}} \phi(\mu) d\mu \right] + \mathcal{U}_{\dot{m}}. \quad (4.11)$$

Since the function ϑ_i is nonnegative, so is $\phi(\rho)$. Moreover, $\rho_{\dot{m}} \in [0, \kappa]$ holds true for every arbitrary point. So, from (4.11), we have

$$\phi(\rho) \leq D \int_0^{\rho} \phi(\mu) d\mu + \mathcal{U}.$$

For $\rho \in [0, \kappa]$, applying Theorem 2.3, we get

$$\phi(\rho) \leq \mathcal{U} e^{D\rho}.$$

More specifically, for $\rho = \rho_{\dot{m}}$,

$$\phi(\rho) \leq \mathcal{U} e^{D\rho_{\dot{m}}},$$

as a result, for $\dot{m} = 0, \dots, \mathcal{M}$, it follows

$$\begin{aligned} \vartheta_{\dot{m}} &\leq \mathcal{U} e^{D\dot{m}\delta} \\ &\leq \mathcal{U} e^{D\mathcal{M}\delta} \\ &\leq \mathcal{U} e^{D\kappa}. \quad \square \end{aligned}$$

Theorem 4.3. Assume that for μ , ϕ , and μ , the twice continuously differentiable functions are \mathfrak{R} and ϕ , respectively. Then the trapezoidal technique (4.7), converges with quadratic convergence to the unique solution of (1.1) only if (E_1) – (E_3) hold.

Proof. Now, for $\rho_{\dot{m}} \in \delta$, applying Lemma 2.5 and the continuity of \mathfrak{R} and ϕ , the following is the form of (4.2):

$$\phi_{\dot{m}} = \varpi_{\dot{m}} + \chi \left(\rho_{\dot{m}}, \frac{1}{\Gamma(\alpha)} \frac{\delta}{2} \sum_{i=0}^{\dot{m}} \left[\frac{\mathfrak{R}(\rho_{\dot{m}}, \rho_{i-1}, \phi(\rho_{i-1}))}{(\rho_{\dot{m}} - \rho_{i-1})^{1-\alpha}} + \frac{\mathfrak{R}(\rho_{\dot{m}}, \rho_i, \phi(\rho_i))}{(\rho_{\dot{m}} - \rho_i)^{1-\alpha}} \right] + \varrho_{\dot{m}} \right), \quad (4.12)$$

where $\varrho_{\dot{m}} = \frac{\delta^2 \rho_{\dot{m}}}{12} \frac{\partial^2}{\partial \mu^2} \mathfrak{R}(\rho_{\dot{m}}, \mu, \phi(\mu)) \Big|_{\mu=\rho_{\dot{m}}} = \mathcal{O}(\delta^2)$, for some $\rho'_{\dot{m}} \in (0, \rho_{\dot{m}})$. Subtracting Eq. (4.7) from (4.12), and utilizing (E_2) and (E_3) in light

of the triangular inequality after applying modulus, we deduce the following

$$\begin{aligned} e_{\dot{m}} &\leq \frac{\gamma_1 \gamma_2}{\Gamma(\alpha)} \frac{\delta}{2} \sum_{i=0}^{\dot{m}} \left[\frac{e_{i-1}}{(\rho_{\dot{m}} - \rho_{i-1})^{1-\alpha}} + \frac{e_i}{(\rho_{\dot{m}} - \rho_i)^{1-\alpha}} \right] + \gamma_1 |\varrho_{\dot{m}}| \\ &\leq \frac{\gamma_1 \gamma_2}{\Gamma(\alpha)} \frac{\delta}{2} \sum_{i=0}^{\dot{m}} \left[\frac{e_{i-1}}{(\rho_{\dot{m}} - \rho_{i-1})^{1-\alpha}} + \frac{e_i}{(\rho_{\dot{m}} - \rho_i)^{1-\alpha}} \right] + \gamma_1 |\varrho|, \end{aligned} \quad (4.13)$$

where $\varrho = \max_{\dot{m}=1, \dots, \mathcal{M}} |\varrho_{\dot{m}}|$, $\dot{m} = 0, \dots, \mathcal{M}$, and $e_{\dot{m}}$ is stated in (4.5).

Now, from Lemma 4.2 and (4.13), we have the following

$$e_{\dot{m}} \leq \gamma_1 \varrho e^{P\kappa}, \quad \dot{m} = 0, \dots, \mathcal{M}, \quad \text{where } P = \frac{\gamma_1 \gamma_2}{\Gamma(\alpha)}.$$

Given that $|\varrho_{\dot{m}}| = \mathcal{O}(\delta^2)$, ϱ corresponds to the same order, and thus the trapezoidal approach has been shown to converge to an order of δ^2 . \square

5. Numerical examples

The discussed methods were employed for a few examples put forth by the study’s authors. The absolute error $e_{\dot{m}}$, which has been determined by (4.5), has been presented in the tables for specific grid points. The tables provide convergence rates for various δ values for the Euler’s and trapezoidal methods. The following are definitions of the \mathcal{L}_{∞} error norm and the corresponding convergence rate η :

$$\|e(\delta)\|_{\infty} := \max \{ |\phi(\rho_i) - \phi_i|, i \in [0, \dot{m}] \},$$

and

$$\eta := \frac{\log(\|e(\delta)\|_{\infty}) - \log(\|e(\frac{\delta}{2})\|_{\infty})}{\log(2)}.$$

Example 5.1. Consider the first example of WSNFVIEs as follows:

$$\phi(\rho) = \varpi(\rho) + \chi \left(\rho, \frac{1}{\Gamma(1/2)} \int_0^{\rho} \frac{\phi^2(\mu)}{(\rho - \mu)^{1/2}} d\mu \right), \quad \rho \in [0, 1], \quad (5.1)$$

where

$$\varpi(\rho) = \rho^{1/2} - \left(\frac{1}{9\Gamma(1/2)} \right) \times \rho^{5/2}$$

and

$$\chi(\rho, \nu) = (\rho \times \nu),$$

with an exact solution $\phi(\rho) = \rho^{1/2}$, and $\alpha = 1/2$. Since $\|\dot{K}\|_{\infty} = 0.1254$, and moreover χ and \mathfrak{R} possess bounded derivatives of first order according to second and third argument respectively, satisfying the assumptions (E_1) – (E_5) with

$$\gamma_1 \geq \max \left\{ \left| \frac{\partial \chi(\rho, \nu)}{\partial \nu} \right| : \rho, \nu \in [0, 1], \nu \in \mathbb{R} \right\} = 0.5000,$$

and

$$\gamma_2 \geq \max \left\{ \left| \frac{\partial \mathfrak{R}(\rho, \mu, \phi)}{\partial \phi} \right| : \rho, \mu \in [0, 1], \phi \in \mathbb{R} \right\} = 0.4900,$$

and $\frac{\gamma_1 \gamma_2 \kappa^{\alpha}}{\Gamma(\alpha+1)} = 0.2765 < 1$. Thus, according to Theorem 3.3, the solution $\phi(\rho) = \rho^{1/2}$ serves as an unique solution to integral equation (5.1). Furthermore, Fig. 1 represents the comparison of the approximate and exact solution of the given example, while as the error for different values of \mathcal{M} as 64 and 256 by two proposed methods is graphically represented by the Figs. 2, 3, 4 and 5. Table 1 compares the errors produced by the two approaches and shows the order of convergence for various values of \mathcal{M} , and is inferred that the errors obtained through the TM are less than those of the EM.

Also, the conditions of Theorem 3.4 hold on $[0, 1]$. So, if we choose $\phi(\rho) = 0$, then

$$\left| \phi(\rho) - \varpi(\rho) - \chi \left(\rho, \frac{1}{\Gamma(\alpha)} \int_0^{\rho} (\rho - \mu)^{(\alpha-1)} \mathfrak{R}(\rho, \mu, \phi(\mu)) d\mu \right) \right|$$

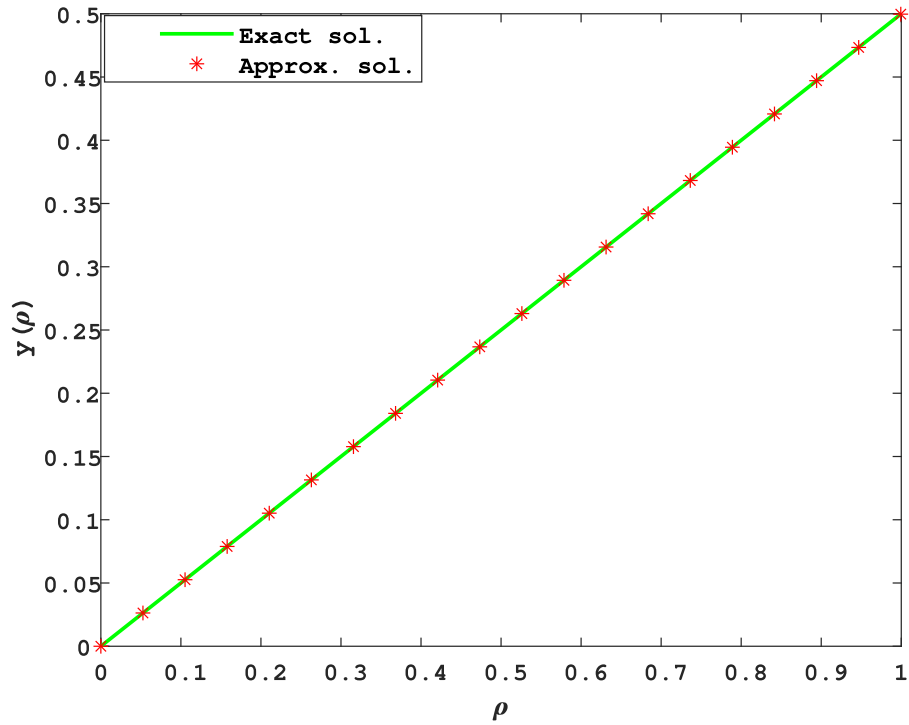


Fig. 1. Exact (Green) and approximate (Red-star) solutions of Example 5.1.

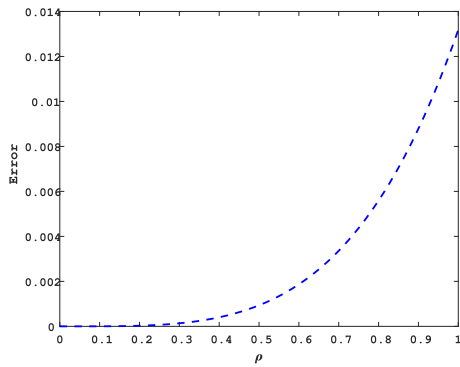


Fig. 2. By EM, the \mathcal{L}_∞ error of Example 5.1, for $\mathcal{M} = 64$.

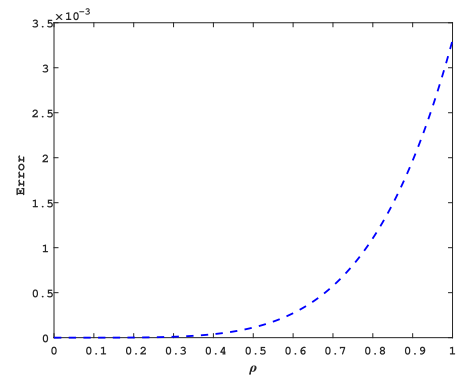


Fig. 4. By EM, the \mathcal{L}_∞ error of Example 5.1, for $\mathcal{M} = 256$.

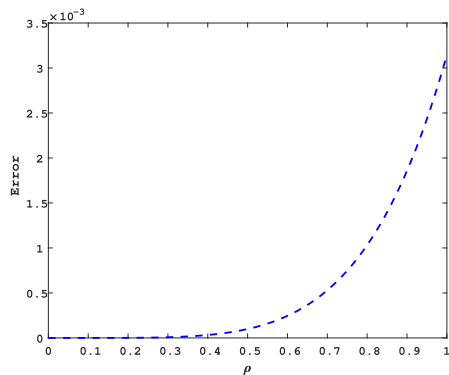


Fig. 3. By TM, the \mathcal{L}_∞ error of Example 5.1, for $\mathcal{M} = 64$.

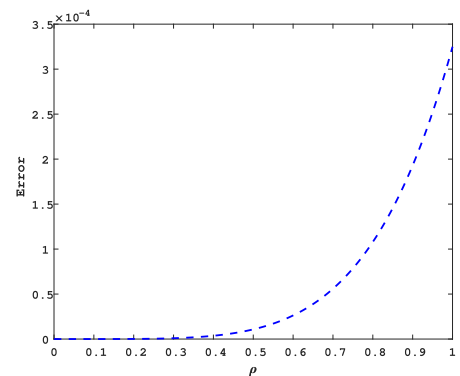


Fig. 5. By TM, the \mathcal{L}_∞ error of Example 5.1, for $\mathcal{M} = 256$.

Table 1
The convergence rates and \mathcal{L}_∞ errors for Example 5.1.

\mathcal{M}	EM		TM	
	$\ e(\delta)\ _\infty$	η	$\ e(\delta)\ _\infty$	η
1	2.7896×10^{-01}	0.8269	1.0972×10^{-01}	1.7361
2	2.7413×10^{-01}	0.8075	1.0852×10^{-01}	1.7806
4	2.6308×10^{-01}	0.8050	1.0528×10^{-01}	1.7987
8	2.4894×10^{-01}	0.9913	7.5785×10^{-02}	1.8124
16	2.2641×10^{-02}	0.9783	9.8045×10^{-03}	1.8574
32	3.4056×10^{-02}	0.9996	9.4018×10^{-03}	1.8841
64	1.3187×10^{-02}	1.0276	3.1447×10^{-03}	1.8901
128	9.4018×10^{-03}	1.0035	9.5828×10^{-04}	1.9149
256	3.3305×10^{-03}	1.0003	3.2491×10^{-04}	1.9919

$$= |0 - \rho^{1/2} - \left(\frac{\rho^{5/2}}{9\Gamma(1/2)}\right) - 0|$$

$$\leq 0.8889 = \epsilon, \quad \forall \rho \in [0, 1].$$

Hence for $\epsilon = 0.08889$, (5.1) has H-U stability follows from Theorem 3.5.

Example 5.2. Consider the second example of WSNFVIEs as follows:

$$\phi(\rho) = \rho^5/2 - \left(\frac{5\pi}{16\Gamma(1/2)}\rho^4\right) + \chi\left(\rho, \frac{1}{\Gamma(1/2)} \int_0^\rho \frac{\phi(\mu)}{(\rho-\mu)^{1/2}} d\mu\right), \quad \rho \in [0, 1],$$

(5.2)

and

$$\chi(\rho, \nu) = (\rho \times \nu),$$

with an exact solution $\phi(\rho) = \rho^{5/2}$ and $\alpha = 1/2$. Since, Example 5.2 satisfies all the suppositions (E₁)–(E₅) with $\|K\|_\infty = 0.5339$, $\left(\frac{\gamma_1 \gamma_2 \kappa^\alpha}{\Gamma(\alpha+1)}\right) = 0.3979 < 1$ and

$$\gamma_1 \geq \max \left\{ \left| \frac{\partial \chi(\rho, \nu)}{\partial \nu} \right| : \rho, \nu \in [0, 1], \nu \in \mathbb{R} \right\} = 1.0000,$$

and

$$\gamma_2 \geq \max \left\{ \left| \frac{\partial \mathfrak{K}(\rho, \mu, \phi)}{\partial \phi} \right| : \rho, \mu \in [0, 1], \phi \in \mathbb{R} \right\} = 0.7052,$$

implying the derivatives of ϕ and χ of first order according to their second and third parameters are bounded. Thus in light of Theorem 3.3, $\phi(\rho) = \rho^{5/2}$ acts as a unique solution of Example 5.2.

The comparison of an actual and the numerically approximated solution of the given example is represented by Fig. 6, while as the Figs. 7, 9 for EM, and Figs. 8, 10 for TM, represent the errors for $\mathcal{M} = 64$ and 256 for the given Example 5.2. In addition to that, Table 2, shows the maximum errors for different values of \mathcal{M} and the convergence order of both methods Euler’s and trapezoidal, which infers that the trapezoidal approach produces less errors compared to the EM.

Also, the conditions of Theorem 3.4 hold on $[0, 1]$. So, if we choose $\phi(\rho) = 0$, then

$$\left| \phi(\rho) - \varpi(\rho) - \chi\left(\rho, \frac{1}{\Gamma(\alpha)} \int_0^\rho (\rho-\mu)^{(\alpha-1)} \mathfrak{K}(\rho, \mu, \phi(\mu)) d\mu\right) \right|$$

$$= |0 - \rho^5/2 - \left(\frac{5\pi\rho^4}{16\Gamma(1/2)}\right) - 0|$$

$$\leq 0.4461 = \epsilon, \quad \forall \rho \in [0, 1].$$

Hence for $\epsilon = 0.4461$, (5.2) has H-U stability follows from Theorem 3.5.

Example 5.3. Consider the third example of WSNFVIEs as follows:

$$\phi(\rho) = \varpi(\rho) + \chi\left(\rho, \frac{1}{\Gamma(1/3)} \int_0^\rho \frac{1}{18} \frac{(\sin^2(\mu) + \phi^2(\mu))}{(\rho-\mu)^{2/3}} d\mu\right), \quad \rho \in [0, \pi/4],$$

(5.3)

Table 2
The convergence rates and \mathcal{L}_∞ errors for Example 5.2.

\mathcal{M}	EM		TM	
	$\ e(\delta)\ _\infty$	η	$\ e(\delta)\ _\infty$	η
1	5.5389×10^{-01}	0.6532	4.0391×10^{-01}	1.7041
2	5.3385×10^{-01}	0.6749	3.5492×10^{-01}	1.7289
4	4.6369×10^{-01}	0.6953	3.0142×10^{-01}	1.7847
8	3.9305×10^{-01}	0.7192	2.1436×10^{-01}	1.7897
16	3.4031×10^{-01}	0.7639	5.5389×10^{-02}	1.8053
32	7.2168×10^{-02}	0.7930	1.5027×10^{-02}	1.8991
64	3.8131×10^{-02}	0.8029	1.5156×10^{-03}	1.9959
128	3.6595×10^{-02}	0.8635	2.9135×10^{-03}	2.0732
256	8.4509×10^{-03}	0.8941	3.7113×10^{-05}	2.0103

Table 3
The convergence rates and \mathcal{L}_∞ errors for Example 5.3.

\mathcal{M}	EM		TM	
	$\ e(\delta)\ _\infty$	η	$\ e(\delta)\ _\infty$	η
1	4.5481×10^{-01}	0.7597	8.2869×10^{-02}	1.6890
2	4.2649×10^{-01}	0.7984	7.6751×10^{-02}	1.8392
4	9.7723×10^{-02}	0.8749	5.4711×10^{-02}	1.8764
8	7.1948×10^{-02}	0.8898	5.0555×10^{-02}	1.8927
16	5.8221×10^{-02}	0.8967	3.8566×10^{-02}	1.9366
32	1.0942×10^{-02}	0.8991	1.3768×10^{-02}	2.0328
64	8.8315×10^{-03}	0.9149	5.3908×10^{-04}	2.0076
128	4.3172×10^{-03}	0.9876	2.7778×10^{-04}	2.0013
256	1.8477×10^{-04}	1.0031	2.8142×10^{-06}	2.0001

where

$$\varpi(\rho) = \cos(\rho) - \left(\frac{\rho^{4/3}}{6\Gamma(1/3)}\right),$$

and

$$\chi(\rho, \nu) = (\rho \times \nu),$$

with an exact solution $\phi(\rho) = \cos(\rho)$ and $\alpha = 1/3$. Since $\|K\|_\infty = 0.0622$, and moreover χ and \mathfrak{K} possess bounded derivatives of first order according to their second and third argument respectively, satisfying the assumptions (E₁)–(E₅) with

$$\gamma_1 \geq \max \left\{ \left| \frac{\partial \chi(\rho, \nu)}{\partial \nu} \right| : \rho, \nu \in [0, 1], \nu \in \mathbb{R} \right\} = 0.0553,$$

and

$$\gamma_2 \geq \max \left\{ \left| \frac{\partial \mathfrak{K}(\rho, \mu, \phi)}{\partial \phi} \right| : \rho, \mu \in [0, 1], \phi \in \mathbb{R} \right\} = 0.0217,$$

and $\frac{\gamma_1 \gamma_2 \kappa^\alpha}{\Gamma(\alpha+1)} = 0.0013 < 1$. Thus, according to Theorem 3.3, the solution $\phi(\rho) = \rho^{1/2}$ serves as a unique solution to integral equation (5.3). Furthermore, Fig. 11 represents the comparison of the approximate and exact solution of the given example, while as the error for different values of $\mathcal{M} = 64$ and 256 by two proposed methods is graphically represented by the Figs. 12, 13, 14 and 15. Table 3 compares the errors produced by the two approaches and shows the order of convergence for various values of \mathcal{M} , and is inferred that the errors obtained through the TM are less than those of the EM.

Also, the conditions of Theorem 3.4 hold on $[0, 1]$. So, if we choose $\phi(\rho) = 0$, then

$$\left| \phi(\rho) - \varpi(\rho) - \chi\left(\rho, \frac{1}{\Gamma(\alpha)} \int_0^\rho (\rho-\mu)^{(\alpha-1)} \mathfrak{K}(\rho, \mu, \phi(\mu)) d\mu\right) \right|$$

$$= |0 - \cos(\rho) - \left(\frac{\rho^{4/3}}{6\Gamma(1/3)}\right) - 0|$$

$$\leq 0.5403 = \epsilon, \quad \forall \rho \in [0, 1].$$

Hence for $\epsilon = 0.5403$, (5.3) has H-U stability follows from Theorem 3.5.

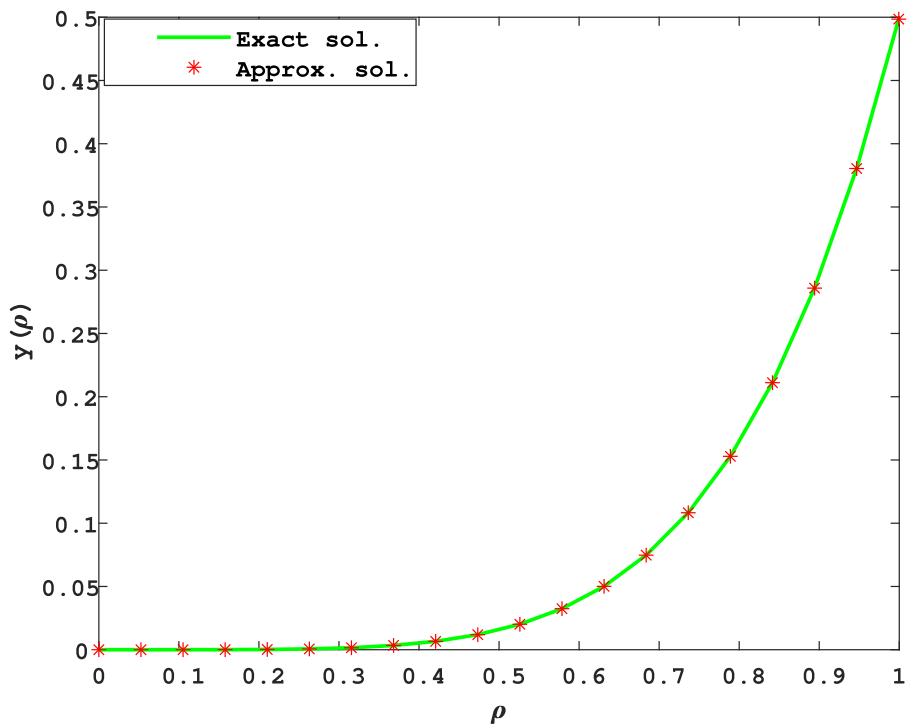


Fig. 6. Exact (Green) and approximate (Red-star) solutions of Example 5.2.

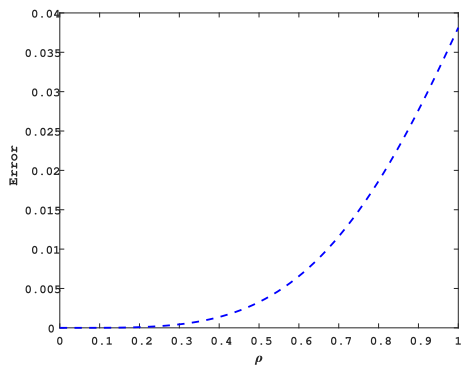


Fig. 7. By EM, the L_∞ error of Example 5.2, for $M = 64$.

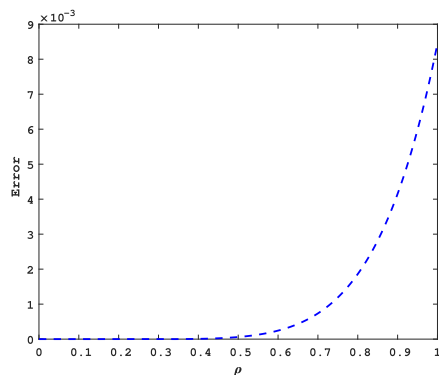


Fig. 9. By EM, the L_∞ error of Example 5.2, for $M = 256$.

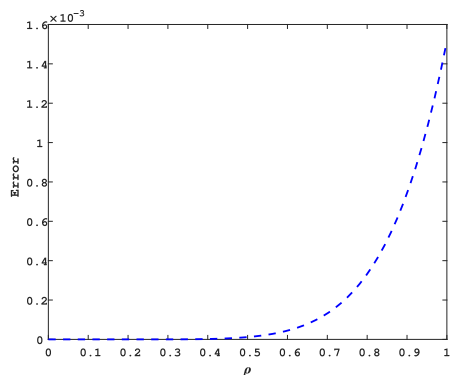


Fig. 8. By TM, the L_∞ error of Example 5.2, for $M = 64$.

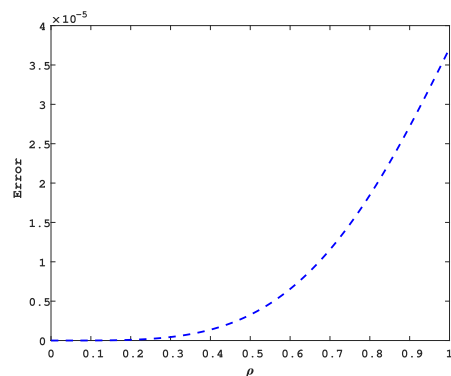


Fig. 10. By TM, the L_∞ error of Example 5.2, for $M = 256$.

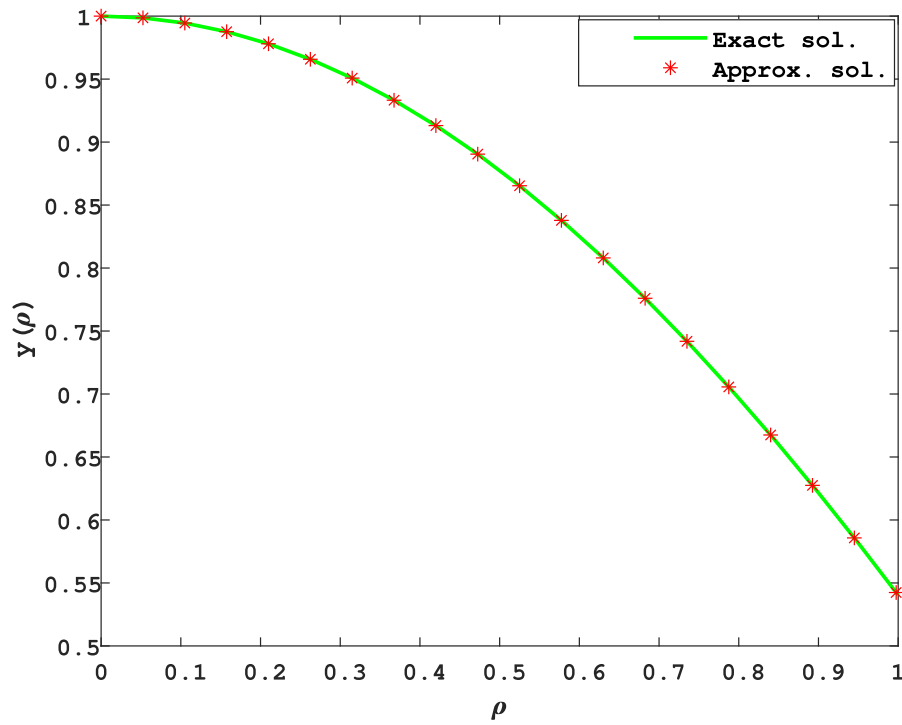


Fig. 11. Exact (Green) and approximate (Red-star) solutions of Example 5.3.

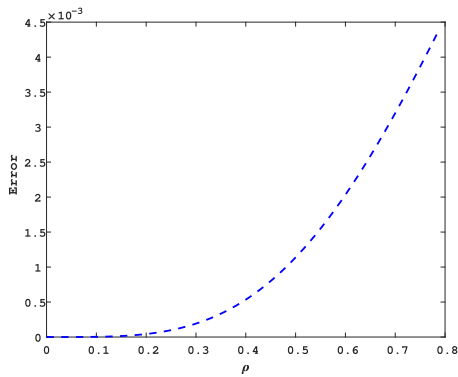


Fig. 12. By EM, the L_∞ error of Example 5.3, for $M = 64$.

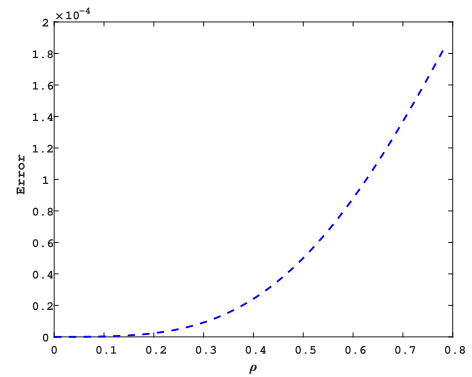


Fig. 14. By EM, the L_∞ error of Example 5.3, for $M = 256$.

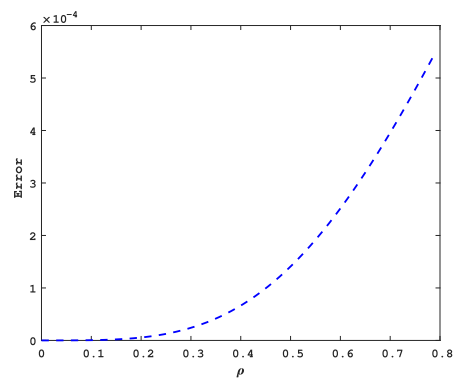


Fig. 13. By TM, the L_∞ error of Example 5.3, for $M = 64$.

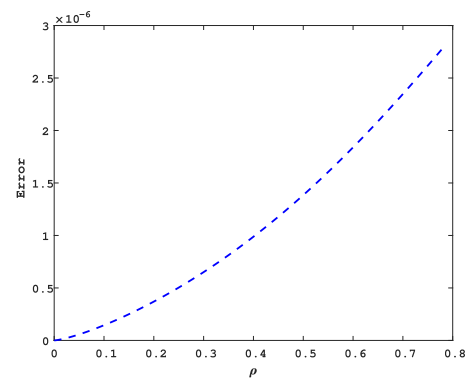


Fig. 15. By TM, the L_∞ error of Example 5.3, for $M = 256$.

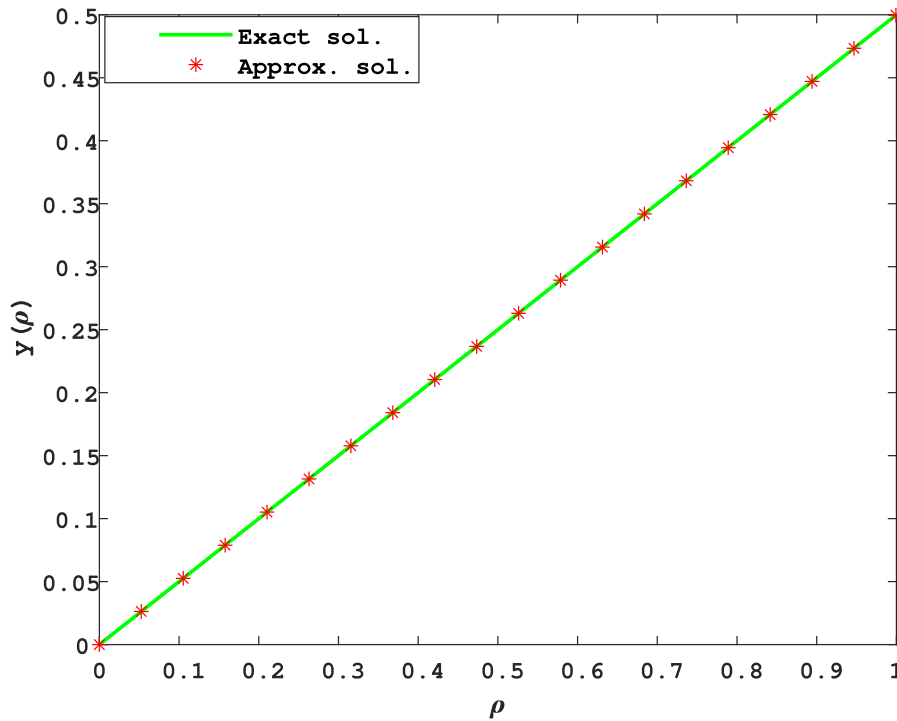


Fig. 16. Exact (Green) and approximate (Red-star) solutions of Example 5.4.

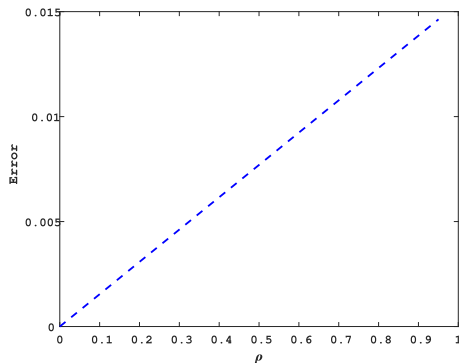


Fig. 17. By EM, the L_∞ error of Example 5.4, for $\mathcal{M} = 64$.

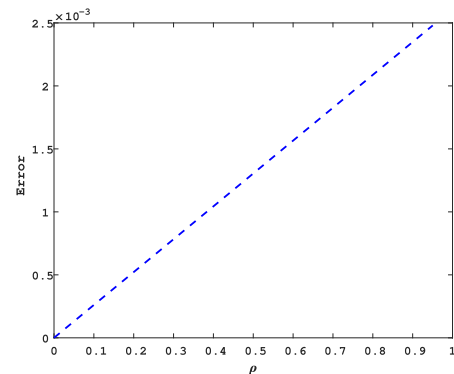


Fig. 18. By TM, the L_∞ error of Example 5.4, for $\mathcal{M} = 64$.

Example 5.4 ([18]). Consider the last example of WSNFVIEs as follows:

$$\phi(\rho) = \rho^{1/2} \left(1 - \frac{1}{\beta^2} \frac{16}{15} \rho^3 \right) + \frac{1}{\beta^2} \int_0^\rho \frac{\rho\mu}{(\rho - \mu)^{1/2}} \phi^2(\mu) d\mu \quad \rho \in [0, 1], \quad (5.4)$$

with an exact solution $\phi(\rho) = \rho^{1/2}$ and $\alpha = 1/2, \beta = 1$. Since, Example 5.4 satisfies all the suppositions $(E_1) - (E_5)$ with $\|\hat{K}\|_\infty = 1.0667, \gamma_1 = 1.5, \gamma_2 = 0.5333$ and $\left(\frac{\gamma_1 \gamma_2 \kappa^\alpha}{\Gamma(\alpha+1)}\right) = 0.9026 < 1$ and implying the derivatives of ϕ and χ of first order according to their second and third parameters are bounded. Thus in light of Theorem 3.3, $\phi(\rho) = \rho^{1/2}$ acts as a unique solution of Example 5.4.

The comparison of an actual and the numerically approximated solution of the given example is represented by Fig. 16, while as the Figs. 17, 19 for EM, and Figs. 18, 20 for TM, represent the errors for $\mathcal{M} = 64$ and 128 for the given Example 5.2. In addition to, Table 4, shows the maximum errors for different values of \mathcal{M} and the convergence order of both methods Euler’s and trapezoidal, which infers that the trapezoidal approach produces less errors compared to the EM. Evidently it is very clear from the Table 4 that comparing the results of (5.4) to the results of [18], the maximum error bound at $\mathcal{M} =$

64, and 128 computed by EM and TM are $1.4632 \times 10^{-2}, 4.1300 \times 10^{-3}$, respectively, very less as compared to that of [18]. Thus our methods give the best approximation to that of the proposed method [18].

Also, the conditions of Theorem 3.4 hold on $[0, 1]$. So, if we choose $\phi(\rho) = 0$, then

$$\begin{aligned} & \left| \phi(\rho) - \varpi(\rho) - \chi \left(\rho, \frac{1}{\Gamma(\alpha)} \int_0^\rho (\rho - \mu)^{(\alpha-1)} \mathfrak{R}(\rho, \mu, \phi(\mu)) d\mu \right) \right| \\ & = \left| 0 - \rho^{1/2} \left(1 - \frac{16}{15} \rho^3 \right) - 0 \right| \\ & \leq 0.0667 = \epsilon, \quad \forall \rho \in [0, 1]. \end{aligned}$$

Hence for $\epsilon = 0.0667$, (5.4) has H-U stability follows from Theorem 3.5.

6. Conclusions

In this sequel, the second kind of weakly singular nonlinear functional Volterra integral Eq. (1.1) of the Urysohn type involving Riemann–Liouville operator has been studied. The equation’s possession of a unique solution under specific Lipschitz conditions on the two

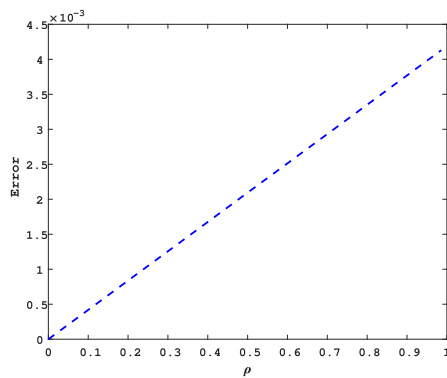


Fig. 19. By EM, the L_∞ error of Example 5.4, for $\mathcal{M} = 128$.

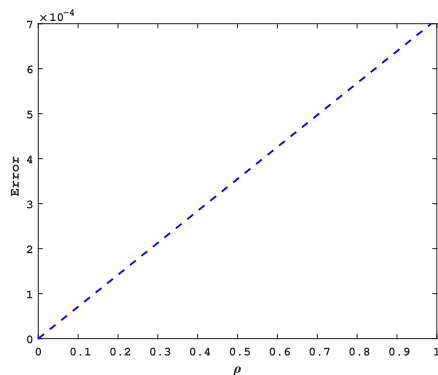


Fig. 20. By TM, the L_∞ error of Example 5.4, for $\mathcal{M} = 128$.

Table 4
Comparing the absolute maximum errors of Example 5.4.

\mathcal{M}	EM		TM		Method in [18] $\ e(\delta)\ _\infty$
	$\ e(\delta)\ _\infty$	η	$\ e(\delta)\ _\infty$	η	
4	1.9984×10^{-1}	0.1089	1.0764×10^{-1}	1.4381	2.1500×10^{-1}
8	1.7360×10^{-1}	0.3614	1.0231×10^{-1}	1.5486	1.6600×10^{-1}
16	1.4880×10^{-1}	0.4832	2.0156×10^{-2}	1.6181	1.2300×10^{-1}
32	5.3085×10^{-2}	0.6484	3.1041×10^{-2}	1.7641	9.0200×10^{-2}
64	1.4632×10^{-2}	0.7841	2.4800×10^{-3}	1.8653	6.5100×10^{-2}
128	4.1300×10^{-3}	0.8362	6.9999×10^{-4}	1.9891	4.6000×10^{-2}

operators involved, the Nemytskii operator and the integral operator, has been demonstrated. In the process of numerical solution approximation, the trapezoidal and Euler discretization methods were employed, leading to the formulation of a nonlinear system of equations. Due to the intricate solvability of this system, confirming the existence and uniqueness of the solution to the ensuing algebraic system posed challenges. Nevertheless, the presented computations indicated that solutions were often attainable, and fixed point approaches yielded reliable approximations. In addition, we determined the H-U-R and H-U stability requirements for solution to the considered integral equation (1.1).

Furthermore, validation occurred that the numerical solution of the discretized system converged to the exact solution of the integral equation, as supported by the application of the Grönwall inequality. Observations from the provided examples revealed quadratic convergence for the trapezoidal method and a first-order convergence rate for the Euler method, aligning with theoretical findings in Section 4. Notably, from the numerical findings presented in tables, it has been inferred that the trapezoidal method consistently outperformed the Euler method by producing the less errors as evidenced by computations conducted using MATLAB 23.2.0.2436196 (R2023b). Additionally, we

contrasted our computational results with the exact solutions of one test case and compared them with outcomes obtained using alternative numerical methods. This comparison showcases the effectiveness of our proposed approaches in relation to methodologies documented in the existing literature [18]. In future, the advanced version of proposed methods will be applied to the weakly singular functional Fredholm integral equations, Caputo fractional-order type models, functional type integro-differential equations, etc.

CRedit authorship contribution statement

Imtiyaz Ahmad Bhat: Conceptualization, Formal analysis, Investigation, Methodology, Software, Validation, Visualization, Writing – original draft, Resources. **Lakshmi Narayan Mishra:** Conceptualization, Formal analysis, Investigation, Methodology, Resources, Software, Supervision, Validation, Visualization, Writing – original draft, Writing – review & editing. **Vishnu Narayan Mishra:** Conceptualization, Formal analysis, Investigation, Methodology, Resources, Software, Validation, Visualization, Writing – review & editing. **Mahmoud Abdel-Aty:** Conceptualization, Formal analysis, Investigation, Methodology, Resources, Software, Validation, Visualization, Writing – review & editing. **Montasir Qasymeh:** Conceptualization, Formal analysis, Funding acquisition, Investigation, Methodology, Resources, Software, Validation, Visualization, Writing – review & editing.

Declaration of competing interest

The authors declare that they have no known competing financial interests or personal relationships that could have appeared to influence the work reported in this paper.

References

- [1] M. Shams, N. Kausar, P. Agarwal, G.I. Oros, Efficient iterative scheme for solving non-linear equations with engineering applications, *Appl. Math. Sci. Eng.* 30 (1) (2022) 708–735.
- [2] M.A. Abdulwasaa, S.V. Kawale, M.S. Abdo, M.D. Albalwi, K. Shah, B. Abdalla, T. Abdeljawad, Statistical and computational analysis for corruption and poverty model using Caputo-type fractional differential equations, *Heliyon* 10 (3) (2024) e25440.
- [3] M. Shams, N. Rafiq, N. Kausar, P. Agarwal, C. Park, N.A. Mir, On iterative techniques for estimating all roots of nonlinear equation and its system with application in differential equation, *Adv. Differ. Equ.* 2021 (1) (2021).
- [4] I. Ahmad, N. Ahmad, K. Shah, T. Abdeljawad, Some appropriate results for the existence theory and numerical solutions of fractals–fractional order malaria disease mathematical model, *Results Control Optim.* 14 (2024) 100386.
- [5] S. Hu, M. Khavanin, W. Zhuang, Integral equations arising in the kinetic theory of gases, *Appl. Anal.* 34 (3) (1989) 261–266.
- [6] K. Shah, B. Abdalla, T. Abdeljawad, M.A. Alqudah, A fractal-fractional order model to study multiple sclerosis: A chronic disease, *Fractals* (2024) 2440010.
- [7] A. Alla Hamou, Z. Hammouch, E. Azroul, P. Agarwal, Monotone iterative technique for solving finite difference systems of time fractional parabolic equations with initial/periodic conditions, *Appl. Numer. Math.* 181 (2022) 561–593.
- [8] P. Agarwal, M. Akbar, R. Nawaz, M. Jleli, Solutions of system of Volterra integro-differential equations using optimal homotopy asymptotic method, *Math. Methods Appl. Sci.* 44 (3) (2020) 2671–2681.
- [9] A. Subhan, K. Shah, S. Subhi Aiadi, N. Mlaiki, F.M. Alotaibi, et al., Analysis of Volterra integrodifferential equations with the fractal-fractional differential operator, *Complexity* 2023 (2023).
- [10] W. Olmstead, R. Handelsman, Diffusion in a semi-infinite region with nonlinear surface dissipation, *SIAM Rev.* 18 (2) (1976) 275–291.
- [11] W.R. Mann, F. Wolf, Heat transfer between solids and gases under nonlinear boundary conditions, *Quart. Appl. Math.* 9 (2) (1951) 163–184.
- [12] P.L. Chambré, A. Acrivos, On chemical surface reactions in laminar boundary layer flows, *J. Appl. Phys.* 27 (11) (1956) 1322–1328.
- [13] W.E. Olmstead, A nonlinear integral equation associated with gas absorption in a liquid, *Math. Phys.* 28 (3) (1977) 513–523.
- [14] K. Kant, G. Nelakanti, Galerkin and multi-Galerkin methods for weakly singular Volterra–Hammerstein integral equations and their convergence analysis, *Comput. Appl. Math.* 39 (2020) 1–28.
- [15] G. Yao, Z. Wang, C. Zhang, A multi-domain hybrid spectral collocation method for nonlinear Volterra integral equations with weakly singular kernel, *J. Comput. Appl. Math.* 444 (2024) 115785.

- [16] S. Micula, A numerical method for weakly singular nonlinear Volterra integral equations of the second kind, *Symmetry* 12 (11) (2020) 1862.
- [17] R. Nigam, K. Kant, B.R. Kumar, G. Nelakanti, Approximation of weakly singular non-linear Volterra–Urysohn integral equations by piecewise polynomial projection methods based on graded mesh, *J. Appl. Anal. Comput.* 13 (3) (2023) 1359–1387.
- [18] O. Baghani, The rate of convergence of an iterative-computational algorithm for second-kind nonlinear Volterra integral equations with weakly singular kernels, *Math. Methods Appl. Sci.* (2020).
- [19] S.K. Paul, L.N. Mishra, V.N. Mishra, D. Baleanu, An effective method for solving nonlinear integral equations involving the Riemann–Liouville fractional operator, *AIMS Math.* 8 (8) (2023) 17448–17469.
- [20] K. Maleknejad, K. Nouri, R. Mollapouras, Existence of solutions for some nonlinear integral equations, *Commun. Nonlinear Sci. Numer. Simul.* 14 (6) (2009) 2559–2564.
- [21] E. Alvarez, C. Lizama, Attractivity for functional Volterra integral equations of convolution type, *J. Comput. Appl. Math.* 301 (2016) 230–240.
- [22] L.N. Mishra, R.P. Agarwal, On existence theorems for some nonlinear functional-integral equations, *Dyn. Syst. Appl.* 25 (3) (2016) 303–320.
- [23] J. Biazar, M.G. Porshokouhi, B. Ghanbari, M.G. Porshokouhi, Numerical solution of functional integral equations by the variational iteration method, *J. Comput. Appl. Math.* 235 (8) (2011) 2581–2585.
- [24] S. Abbasbandy, Application of he’s homotopy perturbation method to functional integral equations, *Chaos Solitons Fractals* 31 (5) (2007) 1243–1247.
- [25] S. Bazm, P. Lima, S. Nemati, Analysis of the Euler and trapezoidal discretization methods for the numerical solution of nonlinear functional Volterra integral equations of Urysohn type, *J. Comput. Appl. Math.* 398 (2021) 113628.
- [26] L.N. Mishra, V.K. Pathak, D. Baleanu, Approximation of solutions for nonlinear functional integral equations, *AIMS Math.* 7 (9) (2022) 17486–17506.
- [27] A. El-Sayed, H.R. Ebead, On the solvability of a self-reference functional and quadratic functional integral equations, *Filomat* 34 (1) (2020) 129–141.
- [28] I.A. Bhat, L.N. Mishra, A comparative study of discretization techniques for augmented Urysohn type nonlinear functional Volterra integral equations and their convergence analysis, *Appl. Math. Comput.* 470 (2024) 128555.
- [29] S. Hassan, M. De la Sen, P. Agarwal, Q. Ali, A. Hussain, A new faster iterative scheme for numerical fixed points estimation of Suzuki’s generalized nonexpansive mappings, *Math. Probl. Eng.* 2020 (2020) 1–9.
- [30] H. Alrabaiah, M. Jamil, K. Shah, R.A. Khan, Existence theory and semi-analytical study of non-linear Volterra fractional integro-differential equations, *Alex. Eng. J.* 59 (6) (2020) 4677–4686.
- [31] A. Ullah, Z. Ullah, T. Abdeljawad, Z. Hammouch, K. Shah, A hybrid method for solving fuzzy Volterra integral equations of separable type kernels, *J. King Saud Univ. Sci.* 33 (1) (2021) 101246.
- [32] S.K. Paul, L.N. Mishra, V.N. Mishra, D. Baleanu, Analysis of mixed type nonlinear Volterra–Fredholm integral equations involving the Erdélyi–Kober fractional operator, *J. King Saud Univ. Sci.* 35 (10) (2023) 102949.
- [33] R. Amin, K. Shah, M. Asif, I. Khan, Efficient numerical technique for solution of delay Volterra–Fredholm integral equations using haar wavelet, *Heliyon* 6 (10) (2020).
- [34] V.K. Pathak, L.N. Mishra, V.N. Mishra, D. Baleanu, On the solvability of mixed-type fractional-order non-linear functional integral equations in the Banach space $C(I)$, *Fractal Fract.* 6 (2022) 744.
- [35] I. Zamanpour, R. Ezzati, Operational matrix method for solving fractional weakly singular 2D partial Volterra integral equations, *J. Comput. Appl. Math.* 419 (2023) 114704.
- [36] I.A. Bhat, L.N. Mishra, V.N. Mishra, C. Tunç, O. Tunç, Precision and efficiency of an interpolation approach to weakly singular integral equations, *Internat. J. Numer. Methods Heat Fluid Flow* 34 (3) (2024) 1479–1499.
- [37] B.G. Pachpatte, *Inequalities for Differential and Integral Equations*, Academic Press, San Diego, 1998.
- [38] P.J. Davis, P. Rabinowitz, *Methods of Numerical Integration*, Courier Corporation, 2007.
- [39] K. Atkinson, *An Introduction To Numerical Analysis*, John Wiley & Sons, 1991.
- [40] A. Karoui, A. Jawahdou, Existence and approximate L^p and continuous solutions of nonlinear integral equations of the Hammerstein and Volterra types, *Appl. Math. Comput.* 216 (7) (2010) 2077–2091.